3D Wavefield Imaging in the Deepwater Gulf of Mexico

Paul Valasek, Kay Dautenhahn Wyatt, Dan Whitmore, Yunqing Shen, Zhaobo Meng, Keith L. Branham, Phillips Petroleum Co.

Summary
When complex structures with large velocity contrasts are present, wavefield techniques can provide improved imaging (structure, amplitude, and phase) over the more traditional Kirchhoff integral methods. Wavefield techniques rely on two elements: firstly, an advanced acquisition design with complete azimuthal coverage; and, secondly, wave equation based prestack imaging methods. Together, these two elements offer improved seismic imaging in complex structural environments by better handling of multipathing, amplitudes and phase. A wavefield experiment was conducted last year in a complex subsalt area of the deepwater Gulf of Mexico using a full-azimuth vertical cable acquisition strategy. Here, we discuss some of the unique challenges associated with wavefield imaging such as velocity analysis and residuals correction. Finally, comparisons will be shown between conventional Kirchhoff imaging and wavefield imaging.

Introduction
Since the early 1990's 3D Kirchhoff prestack depth migration (PSDM) has been used to improve seismic imaging in areas dominated by complex geological structure and strong velocity. The Kirchhoff algorithm has been the oil industry's primary choice for PSDM because of its computational efficiency and its flexibility in handling irregular acquisition geometries. While this method has been successful in improving the imaging compared with conventional 3D seismic processing, there are approximations in this approach that limits its effectiveness in some areas. The primary limitation of Kirchhoff PSDM is the dependence on ray tracing to model the complex seismic wave propagation. The inability of ray theoretical methods to properly model the complete kinematics (traveltimes) and dynamics (amplitudes and phase) of the seismic wavefield can lead to poor focusing and the introduction of migration artifacts beneath complex structures (see Figure 1).

To overcome the limitations of Kirchhoff PSDM, we have developed migration methods that solve the wave equation rather than approximate it. There are several well known depth imaging algorithms that can accomplish this that have, until recently, been too computationally expensive to implement. These wave equation based or wavefield methods directly solve the acoustic wave equation and can properly handle the kinematics and dynamics of the wavefield generated in complex geologic environments (O'Brien, et. al. 1998; Shen et. al., 2000; Meng et. al., 2000). Synthetic data results have demonstrated that this next generation of imaging technology provides improvements in image quality compared with conventional Kirchhoff imaging.

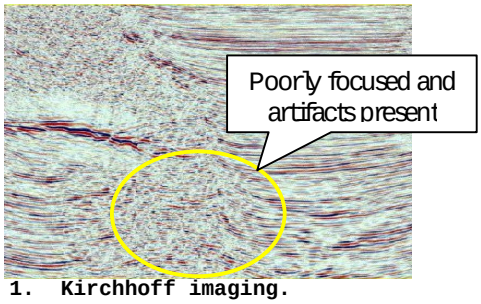

Figure 1. Kirchhoff imaging.

Acquisition Issues in Wavefield Imaging
To take advantage of this new imaging technology, it is preferable to acquire seismic data in a relatively unconventional way. Ocean bottom sensors or vertical cable arrays (Figure 2) with areal acquisition produce 3D common receiver gathers that are suitable for wavefield imaging (after assuming source-receiver reciprocity). Receivers are fixed and separated by several hundreds of meters or up to a kilometer or greater depending on the target depth. These receivers remain stationary for a given shot pattern. The shot pattern is a densely spaced array of shots along the surface. The shot spacing is typically between 50 and 75 meters in both directions. The data are then sorted to common receiver gathers as shown in Figure 3. This data structure or "true" 3D gather is now suitable for wavefield imaging technology.

Wavefield Imaging: Improved Amplitudes
First, we show a synthetic example where wavefield methods produce more reliable amplitudes in subsalt imaging than Kirchoff methods. Figure 4a shows a seismic line over a GOM subsalt prospect. A model was constructed from the seismic data and a low velocity lens was added beneath the salt to more adequately evaluate the ability of wavefield imaging to reconstruct accurate seismic amplitudes. Synthetic, finite difference acoustic data was generated from this model and subsequently input to both Kirchhoff prestack depth migration (Figure 4b) and wavefield imaging (Figure 4c).

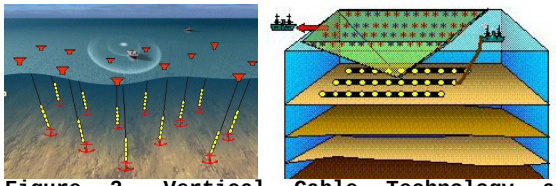

Figure 2. Vertical Cable Technology and ocean bottom sensors are examples of the type of marine acquisition geometry suitable for wavefield imaging.

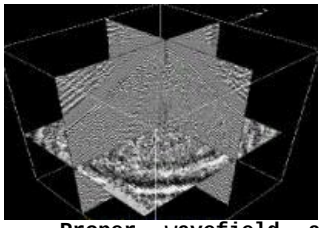

Figure 3. Proper wavefield acquisition results in a collection of full-azimuth common receiver gathers.

At first glance, both Kirchhoff and wavefield results look similar. However, a closer look reveals differences in their ability to recover accurate amplitudes. Figure 5 shows an enlarged version of the imaging near the low velocity lens. Here we see the value of wavefield imaging for providing improved seismic amplitudes below salt. The conventional Kirchhoff imaging does not produce amplitudes that correctly represent the seismic reflectivity associated with the velocity model. The Kirchhoff amplitudes vary laterally and are smeared at the edges of the lens. On the other hand, the amplitudes produced by wavefield imaging are uniform and sharply focused at the edge of the lens.

Wavefield Imaging for Improved Structure Below Salt

Next, we show an example where wavefield imaging can improve the structure in subsalt imaging. Figure 6a shows a second line over this same prospect in the GOM. In this case, significant distortion is seen below the rugose salt and at the boundaries of the salt sills. We have generated a velocity model and synthetic data in a similar fashion to the example shown in Figure 4.

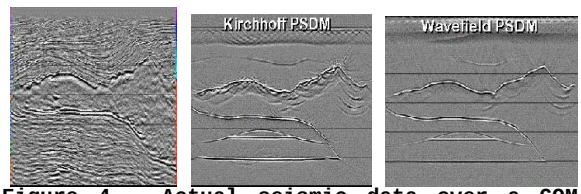

Figure 4. Actual seismic data over a GOM subsalt prospect (a), a Kirchhoff prestack depth migration (PSDM) on the synthetic seismic data (b), and wavefield imaging of the synthetic data (c).

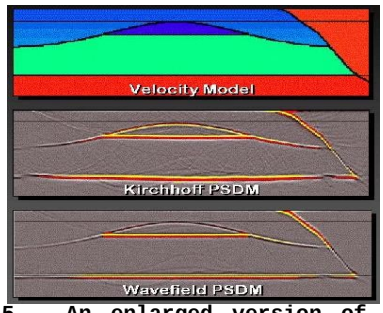

Figure 5. An enlarged version of the low velocity anomaly from Figure 4.

The Kirchhoff PSDM image of the lens structure exhibits numerous artifacts, particularly beneath the sediment window. The amplitudes of the lower flat event, as well as its structure have significant errors. In the wavefield PSDM, however, the event structure and amplitudes are significantly improved

An enlarged version of the low velocity lens area shows the significant improvements in image quality obtained with wavefield imaging over the Kirchhoff PSDM (Figure 7).

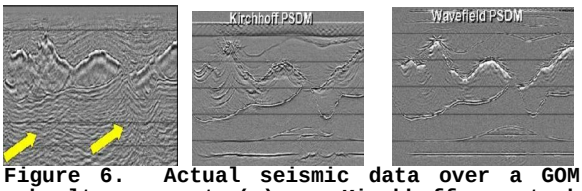

Figure 6. Actual seismic data over a GOM subsalt prospect (a), a Kirchhoff prestack depth migration (PSDM) on the synthetic seismic data (b), and wavefield imaging of the synthetic data (c).

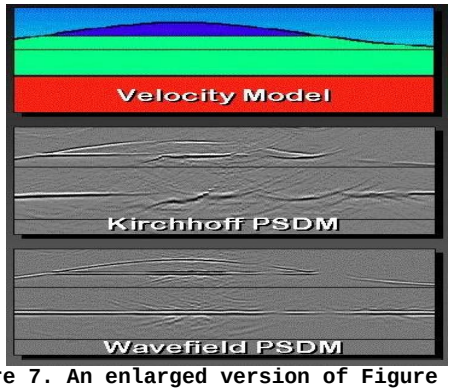

Figure 7. An enlarged version of Figure 6.

Vertical Cable Field Experiment

A vertical cable seismic survey was acquired in the deepwater Gulf of Mexico during the summer of 1999 using wavefield acquisition geometry (Krail, 1994). The survey was acquired over the salt body shown in Figure 8 in water depths ranging from 800 to 1000m. Thirty-two vertical cables were deployed for the duration of the acquisition

using a staggered grid. Maximum offsets used in the processing reached 7 km.

Each vertical cable had 16 hydrophone levels. A vertical slice through one common receiver gather is shown in Figure 9. Each common receiver gather was 12km on a side. The true 3D geometry of the gathers permits application of advanced pre-migration processing algorithms such as 3D wave equation demultiple.

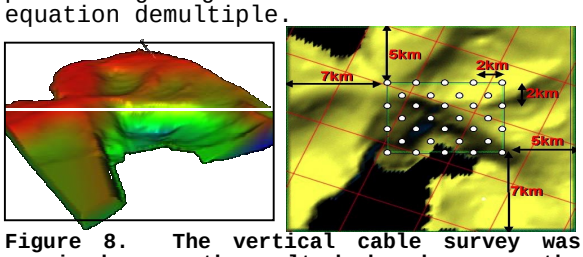

Figure 8. The vertical cable survey was acquired over the salt body shown on the left. On the right is the acquisition geometry for the 32 vertical cables.

By separating the total wavefield into direct (upgoing) and mirror (downgoing) wavefields, we then have 512x2 or 1024 common receiver gathers available for wavefield imaging. In general, the mirror wavefield provides the more optimal image in the shallow portion of the data because of the expanded reflection point coverage (see Figure 10).

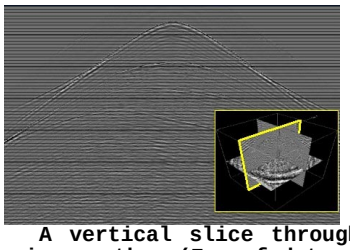

Figure 9. A vertical slice through the 3D common receiver gather (7 s of data shown).

Challenges in Wavefield Imaging

Wavefield imaging is applied to each common receiver gather in a reciprocal shot fashion, and then composited to form a final image. One of the greatest challenges in wavefield imaging is velocity analysis and the application of residual corrections (post-imaging) prior to compositing. Because of the coarse receiver array, conventional methods can not be used to obtain a velocity model directly from the vertical cable data. In this case, a starting velocity model was available from streamer data acquired previously over the area where the vertical cable survey was acquired.

Unlike Kirchhoff PSDM that is typically applied to common offset data, wavefield imaging is applied to common receiver gathers. After imaging, all offset information is lost since all offsets (for that receiver position) are migrated into a single image. Thus, when common image gather (CIG) data are formed for a given image location, we cannot sort by offset for velocity analysis and residuals application. The data can be sorted in a pseudo-offset fashion by using the distance from image point to receiver location. This proves adequate for flat reflectors, but when dip is present, the appearance of these CIGs does not result in the typical moveout behavior of common offset migration techniques such as Kirchhoff PSDM as shown in Figure 11. This makes velocity analysis and the applications of residuals very difficult.

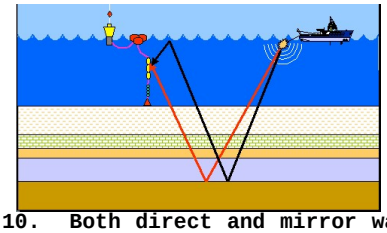

Figure 10. Both direct and mirror wavefield data are used in the wavefield imaging.

One possible solution is to remap a wavefield CIG to an offset sorted CIG using specular raytracing to calculate the actual offset. After the remap procedure, more conventional velocity analysis and residuals application can be applied.

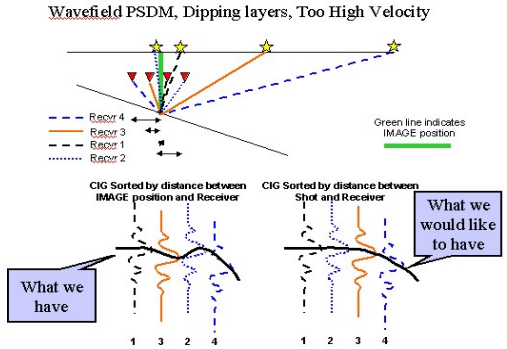

Figure 11. Velocity analysis and residual corrections are more challenging for wavefield imaging

For this study, a velocity model was available which was generated from prestack analysis of streamer data. Wavefield imaging using both 3D Hale-McClellan PSDM (Meng, et. al., 2000) and 3D reverse-time prestack migration (Shen, et. al., 2000) were applied to both the up and downgoing vertical cable wavefields. In general, the RTM images had better definition of the steep dips, whereas the Hale-McClellan images provided better vertical resolution. Figure 12 shows a representative comparison between Kirchhoff and wavefield imaging of vertical cable data. The complex salt body produces significant multi-pathing that is not

properly handled by Kirchhoff imaging. In contrast, the wavefield imaging produces improved continuity of subsalt reflections.

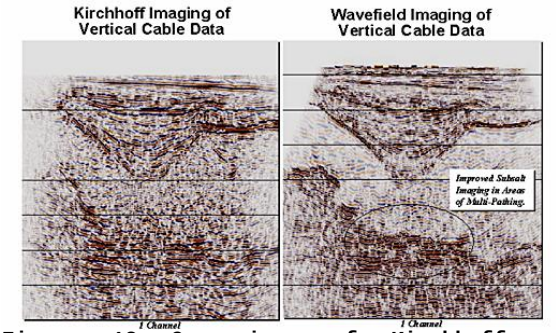

Figure 12 Comparison of Kirchhoff and wavefield imaging of vertical cable data

Conclusions

Wavefield imaging is a promising technique for imaging targets in complex velocity structures. The full-azimuth coverage of the input seismic data, together with the wavefield imaging step which more accurately honors the wave equation produces improved images compared with conventional Kirchhoff 3D PSDM. Wavefield imaging does pose more challenges in acquisition design, computational requirements, velocity model estimation and the application of residuals. Both synthetic data and vertical cable data acquired in the deepwater GOM are used to illustrate these concepts and to show the potential benefits of this technology over that of conventional Kirchhoff PSDM.

Acknowledgements

We also wish to thank the Phillips Petroleum Co. deepwater exploration team for their support of this research and for allowing us to publish this work.

.

References

Krail, P. M., 1994, Vertical cable as a subsalt imaging tool: The Leading Edge, 13, no. 08, 885-887.

Meng, Z., Whitmore, N.D., Valasek, P.A., Shen, Y., Wyatt, K.D., and Liu, W., 2000, 3-D Hale-McClellan prestack depth migration with enhanced extrapolation operators: 70th Ann. Internat. Mtg.: SEG, 485-488.

O'Brien, M.J. and Etgen, J., 1998, Wavefield imaging of complex structures with sparse, point-receiver data: 68th Ann. Internat. Mtg: SEG, 1365-1368.

Shen, Yunqing, Valasek, Paul A., Kelly, Ken, Whitmore, N. Daniel, Wyatt, Kay D., 2000, 3-D prestack reverse-time depth migration with vertical cable data: 70th Ann. Internat. Mtg.: SEG, 762-765.

A Deepwater Pore Pressure Risk Management Case in Offshore Brazil

William L. Abriel, Dieter Letsch, Mike Luken, Stan Teerman*
Chevron Petroleum Technology Company, San Ramon, California
Jay Bruton,
Chevron Petroleum Technology Company, Houston, Texas

Abstract

A well was planned as the first in the deepwater Cumuraxitiba basin offshore Brasil. The well casing and the mud program were designed for abnormal pressure based on risk from offset wells on the shelf and a seismic velocity model. Interval probability analysis illustrated an opportunity to decrease the uncertainty of this risk.

Basin modeling and seismic tomography were performed and uncertainty was reduced, pointing to the probability of a normally pressured well. The well design was altered reducing cost, and the subsequent drilling of the well has confirmed the normal pressure prediction.

Introduction

Earlier this year in offshore Brasil, a well was designed for deepwater exploration. Wells have been drilled in this basin on the shelf, but this was the first well designed to drill in deep water. The casing and drilling mud program were designed in anticipation of abnormal pressure.

The risk of abnormal pressure is uncertain in undrilled areas, as pressure mechanisms and valid pore pressure profiles are not available for calibration. This is a measure of lack of information and not true negative risk. In the case we are addressing, a pressure study based on seismic velocity pointed to abnormal pressure at the chosen drill location. Prior drilling on the shelf exhibited both normally and abnormally pressured conditions. It is therefore reasonable that the design for the first well in the deep-water part of the basin was designed for abnormal pressure.

High levels of uncertainty in pressure prediction can lead to expensive well designs to ensure the ability to reach the objective depth. To address this perceived risk of meeting the exploration objective, the mud weights are elevated, and the casing program is larger and more expensive.

Description of risk in drilling varies within and between companies. Unlike the description of geological risk and reserves uncertainty (Otis et. al. 1997), there exists no similar industry consistent process for describing and associating drilling risks in the presence of abnormal pressure. In this paper, we use a risk description employing interval uncertainty calculus (Davis et. al., 2000) that does not rely on Gaussian assumptions for risk assessment. This is especially useful in areas with limited data or experience, where prior probability data required by Gaussian methods cannot be obtained. For a properly posed process, the interval probability calculus utilizes independent and interdependent data both in favor and against the question at hand.

Pressure Prediction and Interval Risk Analysis

In the Cumuraxitiba basin, the pore pressure prediction practice was employed utilizing analogue wells, a compaction model, and 2D DMO seismic velocity. The well closest to the deepwater part of the basin did not show abnormal pressure, but another well nearby did. The high pressure experienced in the basin is important, and it is necessary to put this into context with other available data. The evidence for and against pressure using the analogue wells alone can be shown with interval probability (figure 1, the cell labeled “analogue wells”). There is some evidence in favor of a normally pressured well (estimated at p= .34 in favor; green) and some evidence for a high pressure well (p= .17 against; red). The largest probability in simply the unknown (p= .49 uncertain; white).

Pressure prediction from well data alone is not sufficient in this case, as the prospect to be drilled is far from the prior wells, and may represent a different geological history. It is known that seismic data can be useful to predict pressure (Dodds et. al. 2001). 3D seismic interpretations of important geological horizons were converted to depth, and a grid of 2D dip-moveout velocity was smoothed and employed in pressure prediction. A compaction profile mechanism was employed to then interpret the data against the fracture gradient. The results show an abnormally high-pressure cell in the area of drilling interest (figure 2). An interval probability measure of this (figure 1, labeled “seismic velocity”) shows significant negative probability for drilling a normally pressured well (p= .46; red) and yet a significant degree of uncertainty (p= .49; white).

Combination of the both analogue well data and the seismic pressure model in an interval probability analysis shows that the favorable evidence for a normally pressured well is significantly countered by negative data from both the high pressure analogue well and the negative information of the seismic pressure model. Total probability (figure 1, top cell) against a normally pressured well (p= .33) is greater than probability in favor (p= .27). Of significance, is

the size of uncertainty (p= .40) in the analysis. It is easy to see that this high level of negative information plus uncertainty leads to a design of the well that is required to handle abnormal pressure.

Reducing the Uncertainty

Can this uncertainty be reduced? As posed, there are two estimation branches of contributing processes to describe pressure prediction – the well analogues and the pressure modeling.

The evidence of high pressure from the analogue wells is conflicting. In this risk model, the wells are considered independent, with the closer well contributing twice the significance of the high pressured well farther away. Reduction of uncertainty in this branch of the risk description, as posed, can only be improved with more drilling.

The evidence of high pressure from the modeling branch however, might be improved through further work. Items that could be better considered include 1) identification of the over-pressure mechanism, 2) detail of the geological model, and 3) precision of the velocity analysis.

Review of Geological and Geophysical Data

From wells on the shelf, it is known that the lithology of the upper part of the section contains significant carbonate. Below this, the wells penetrated older sands and shales with limited porosity. The lithology of the deepwater equivalents of these units must be inferred from a basin-scale geological model, seismic reflection patterns and seismic velocity data. The interpretation of these data is that the carbonate wedge is not present in the deep water.

Seismic reflections from the deepwater also show that the basin has undergone both extensional and compressional tectonic events. In addition, The inferred depositional history shows significant unconformities and some removal of overburden. Regional knowledge points to likely hydrocarbon generation at depth and possibly cementation events that also need to be factored into the pressure prediction.

These data elements of the geology argue for additional basin modeling for predicting tectonic and diagenetic pressure effects and fluid flow history. Tectonic pressure prediction risk (i.e. fault transmission) and expulsion/cementation diagenetic modeling were included in the analysis for pressure to supplement the analogue and seismic prediction processes.

A review of the seismic velocity pressure prediction process suggests that this also could be improved. 2D stacking velocity and interval velocity are variable indicators of true rock velocity in structurally complex areas such as this. These 2D velocity data were analyzed for areal variations, and found to be unreliable for pressure prediction requirements. Significant velocity mis-ties at intersecting lines point to the degree of instability of the measurements.

The pressure uncertainty is highly dependent on the accuracy of the velocity measurements. Therefor, a velocity model for the basin was constructed using state-of-the-art velocity analysis (tomography and depth imaging) on seismic lines, and subsequently building a 3D model from these plus the well velocity data (figure 3).

Pressure Modeling Results

The results of basin modeling and seismic pressure modeling contributed to a different perception of the risk. From the basin modeling, it became apparent that expulsion of hydrocarbons had little effect on the pressure history. This was also found to be true for the erosion and cementation effects. Unfortunately, very little could be predicted about tectonic pressure effects.

The seismic model was significantly altered with the use of tomography measurements. Confidence in the tomographic velocity model was high due to its consistency, precision, and conformity to the geological model. Inversions of the velocity field to pseudo-sonic profiles were a good fit to the geological model of the basin and the seismic pattern analysis of facies.

For specific potential well sites, the pressure model was consistent with the low-pressure well drilled on the shelf. A comparison of the sonic log of this well and the pseudo-sonics of the proposed well sites (figure 4) shows a good fit at depth below the carbonate wedge which does not extend beyond the shelf (figure 3). The low-pressure analogue well has a very simple pressure history with leak-off tests and mud weights that are significantly less than the fracture gradient of the formations.

Potential well site pressure predictions were then made with this geological and geophysical model. Two compaction trends were interpreted at depth with a major velocity slope change at a major unconformity. This dual compaction model then predicts very normal pressures well below the fracture gradient calculated from Gardner's relation of density from velocity. This changed the perceived risk of abnormal pressure for the proposed well site.

Revised Risk Analysis

The interval probability risk analysis of the pressure prediction was useful by evaluating many different types of evidence from non-Gaussian processes. The risk tree was built with two main branches – well analogues and pressure models (figure 5).

The seismic pressure model is a strong contributor (estimated to be 90% sufficient for pressure modeling) to the risk evaluation. These data are high indicators of a normally pressured well, with evidence estimated at 66% in favor and 24% unknown.

The high-pressure analogue well shows evidence against a normally pressured well in the deep basin (85% against and 15% unknown). However, this does not overcome the positive evidence of the other analogue well and the seismic-based pressure model.

The evidences in favor, against, their sufficiency, and their interdependence are all used in computing the pressure risk at the top of the tree. Predicted pressure of the well site to be drilled is considered to have 56% positive evidence for normal pressure (green), 17% evidence of high pressure (red), and 27% unknown (white). If the unknown is considered equally likely to be positive or negative, then the chances of drilling a normally pressured well are 70%.

Impact on Well Program

The revised prediction of drilling a normally pressured was considered to be favorable enough to consider a slim-hole design. The well casing and mud weight program were significantly reduced resulting in a much lower overall cost.

Although the probability of a normally pressured well was considered to be only 70%, the lower cost was a compelling business driver to approve drilling with a slim-hole program plus sufficient contingencies to ensure safety. There has been good news regarding the pressure predictions for this well. The well was successfully drilled to the objective section with the low-pressure well design and encountered normal pressure.

The impact of the revision of the pressure prediction risk was to significantly reduce the design cost of the well. In this somewhat expensive deep water well, the design cost was reduced by at least 25%. Additional designs of wells to be drilled in the basin are now also much less expensive.

Conclusions

Pore pressure prediction in new basins is a very model dependent process. Gaussian probability analysis is not helpful in assessing this risk, as no prior probabilities exist. Offset analogue wells, basin modeling and seismic pressure modeling can all contribute effectively to risk estimates of pressure by employing interval probability analysis that relaxes the assumptions of Gaussian methods.

References

Davis, J. P., and Fletcher, A. J. P., 2000: Managing assets under uncertainty, SPE paper 59443.

Dodds, K, Fletcher, A., Bekele, E., Henning, A. Johnson, M., Abriel, W., Higgs, W., and Strudley, A., 2001: An overpressure case -history using a novel risk analysis, APEA,

Otis, Robert M., and Schneidermann, Nahum, 1997: A process for evaluating exploration prospects: AAPG Bulletin, V. 81, No. 7, 1087-1109.

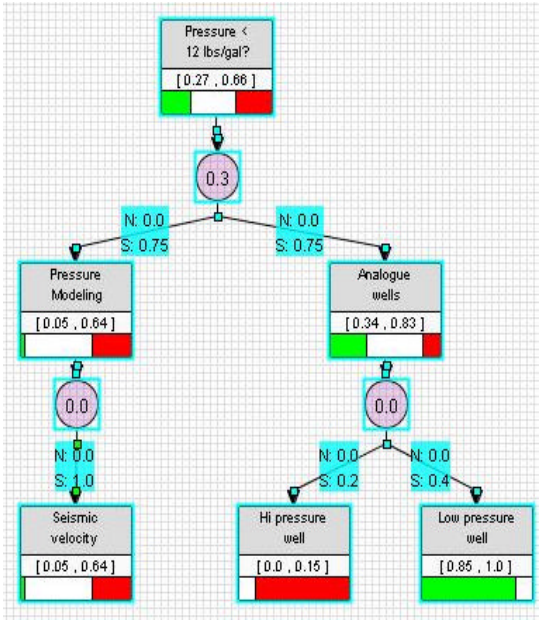

Figure 1 - Interval probability analysis of normal pressure risk based on analogue wells and 2D DMO seismic velocity analyses.

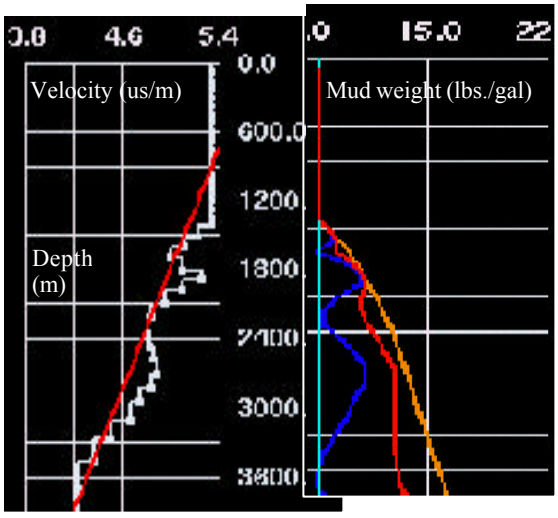

Figure 2 - Velocity and pore pressure estimates based on 2D DMO seismic velocity analyses.

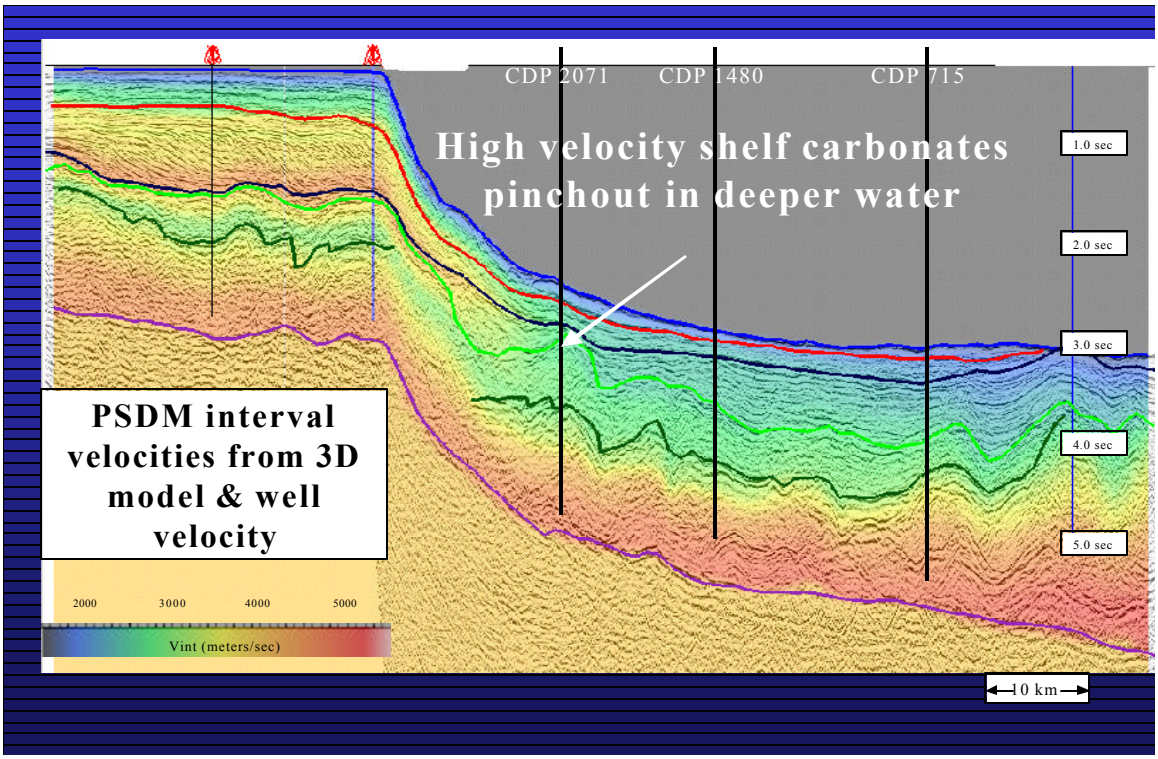

Figure 3. Seismic section and velocity based on tomography.

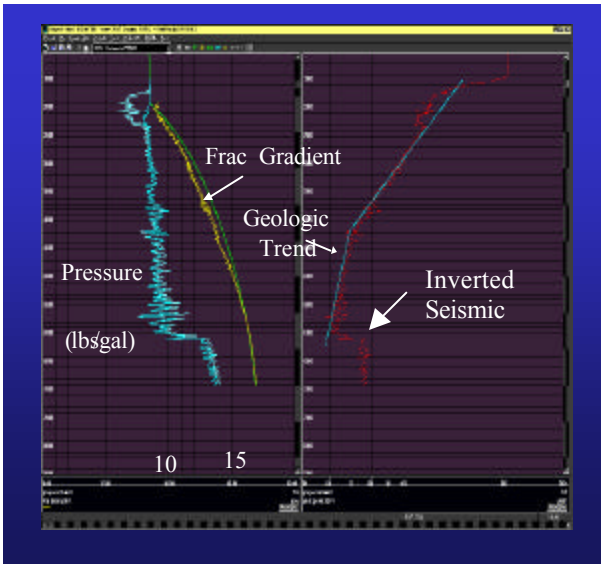

Figure 4. Pore pressure analysis based on inverted tomographic velocity analyses.

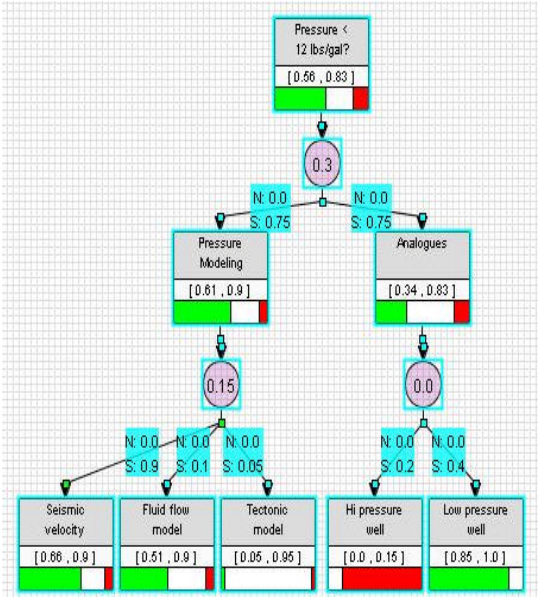

Figure 5. Interval probability analysis based on seismic tomography, basin modeling and analogue wells.

Mantle-Plume-Generated Triple Junction between NE Brazil and West Africa?

Renato M. Darros de Matos, UFRN, Brazil

Abstract

This paper has three purposes. First, it offers an overview of the nature and history of the interior and offshore basins of Northeast Brazil and West Africa, and their relationship to the development of the Southern and Equatorial branches of the Atlantic. Second, it places emphasis on the differences of the rift systems and the control exercised by basement structures on the conjugate margins of West Africa and Northeast Brazil. Third, as the most important, it challenges the idea of a mantle-plume-generated triple junction between Northeast Brazil and West Africa.The Benue Trough is very often cited as one of the best examples of a failed arm of an RRR triple junction (Burke and Wilson, 1976), formed through the activation of a mantle plume. This would imply in: (1) early crustal doming, warping and flexure over a plume with crestal alkaline volcanoes; (2) formation of three simultaneous rift arms, symmetrically orientated at 120^0 to each other; (3) if one rift arm is aborted, the other two develop into a single ridge (new margin) and drift begin; and (4) growth of delta at the mouth of a failed arm. Among them, just the last one is corroborated by the data set. Voluminous magmatism clearly post-dated the opening of the Equatorial Atlantic. Rifting and drifting were diachronous among the African - Brazilian basins and the rift arms are not symmetrically orientated, and finally, instead of one, there are two failed arms: Benue Trough and the onshore Potiguar basin.

Introduction

The West African basins and the Northeast Brazilian rift system (NBRS) yield critical data to understand how continental fragmentation varies through space and time. This fragmentation was recorded as a series of initially intercontinental rift basins associated with the intersection of the **Southern** and **Equatorial** branches of the Atlantic rift system (Figure 1). Based on changes in structural style, facies association, deformation rates, and duration of subsidence, three synrift phases are recognized in the northern tip of the **Southern Branch**, namely Syn-rift I, IIa, IIb and III (Matos, 1999a, Table 1). Most of the extensional events are marked by the widespread occurrence of tilted half-grabens distributed within three main rift axes: (1) the Gabon-Sergipe Alagoas (GSA) trend, (2) the Recôncavo-Tucano-Jatobá (RTJ) trend and (3) the Cariri-Potiguar (CP) trend. The Syn-Rift I sequence, which is often referred to as a pre-rift section, encompasses late Jurassic-early Berriasian clastics that filled the broad shallow "African-Brazilian Depression". The main rift stage (Syn-Rift II, Neocomian-early Berriasian) resulted in widespread block faulting over the GSA, RTJ and CP trends. It is defined by sets of asymmetric half-grabens separated by basement highs, transfer faults, and/or accommodation zones. A general NNW-SSE tectonic transport direction is consistent with the development of the NE-SW half-graben sets throughout the Borborema Province. The late Barremian sediments (Syn-Rift III) document a major change in rifting kinematics, related to the synchronous development of two deformational trends: the onset of stretching at the equatorial branch and higher extensional rates at the GSA trend. Extensional deformation became more focused, and the direction of tectonic transport switched from NNW (Syn-Rift II-b) to a roughly EW direction (with respect to South America). The CP trend was aborted, stretching was initiated at the Equatorial branch-Benue trough, and the southern branch entered its main stretching phase with the accumulation of thick syn-rift section in the Gabon and Sergipe-Alagoas basins. The Equatorial fragmentation process climaxed during the Aptian, when an almost instantaneous extension was responsible for the widespread fracturing of the **Equatorial Atlantic**, generating relatively wide and shallow precursory basins, with no evidence of volcanic margins or widespread development of typical syn-rift basins, as expected in orthogonal extensional regimes. The equatorial splitting evolved during the Albian-Cenomanian interval, through a multi-stage basin development, which is better understood if the kinematics and dynamic controls are considered along with the chronological activation of transform faults, the emplacement of oceanic crust and the onset of drifting between Africa and South America (Matos, 1999b). The geodynamic evolution on the Equatorial Atlantic is addressed by recognizing tectonic stages that pre-date, are synchronous or post-date the activation of transform faults in the Equatorial Atlantic (Matos, 1999b, Table 2).

The Transversal Zone: A key feature between NE Brazil and W Africa

The “Transversal Zone” make-up a roughly orthogonal structure, spreading between the Pernambuco- Ngaundere shear zone and the Benue Trough (Africa) -Touros High (Brazil, Figure 1). The site of lithospheric rupturing does not seem to have followed

any previous upper crustal weakness, especially within the Transversal Zone; even though rifting architecture in NE Brazil and West Africa were controlled by the Braziliano/Pan African heritage. This Transversal Zone had a unique evolution defined by a very fast stretching phase (~5 My) during the Aptian time, responsible for overcoming the last tectonic link between Africa and Brazil. A roughly linear hinge zone denotes localized deformation, induced by a focused lithospheric thinning, resulting in a transient thermal anomaly and minor localized topographic uplift. The Transversal Zone is quite orthogonal to the proto-Equatorial Atlantic, and does not corroborate the idea of a triple junction between the Touros High (Brazil) and Benue Trough in Africa. Rifting is diachronous. The Neocomian-Barremian onshore Potiguar basin, strongly controlled by upper crustal heterogeneity (Matos, 1999), predates the opening of Benue Trough (Aptian), which was not significantly influenced by the Proterozoic heritage, indicating different processes of lithospheric thinning between the Equatorial and the Southern branches.

Transform vs. Divergent Margin Segments

Major differences are observed between the transform and the divergent margin segments of the South Atlantic. In the Southern branch rift architecture is commonly defined by tilted half-grabens, with depocenters controlled by planar/listric faults, and filled with a divergent wedge of siliciclastics sediments, not promptly recognized in the Equatorial margin domain. Sedimentary basin development in oblique/transform settings is less understood than in extensional/divergent settings. The Equatorial Atlantic Margin, which provide a very good example of an ancient transform margin was developed under the kinematic influence of the St. Paul, Romanche and Chain Fracture Zones.

Magmatism

Magmatism in the Benue trough is older, and are represented by the Burashika volcanic complex (147 + 7 Ma, K/Ar, Popoff et al., 1988) and earlier granitic intrusions of the Jos Plateau (Nigeria), with Triassic-Jurassic ages (213 to 141 Ma Rb-Sr, Vail, 1989). Voluminous magmatism clearly post-dates the opening of the Equatorial Atlantic. Pre and syn rift magmatism in NE Brazil are confined to a dike swarm, known as the Rio Ceará Mirim Magmatism (K/Ar ages ranging between 150 and 120 Ma, Upper Jurassic – Neocomian). The idea of a hot spot (St. Helena) triggering the onset of rifting in the Equatorial Atlantic (O'Connor and Duncan, 1990) is controversial because true evidence for an active hot spot in the region comes only from the Tertiary record. In order to add corroborative evidence for an active plume system, some authors have considered magmatic data from distant basins, such as the Cabo basin (Wilson and Guiraud, 1992). However, this basin is located about 500 km away from the Potiguar-Benue junction. These data would suggest a very broad zone of diffuse volcanism, and might provide evidence for a quite broad "mushroom head" or extensive underplating. The issue is not whether we have enough evidence for an ancient cold weak plume, but whether it was strong enough to trigger rifting or it just weakened the lithosphere, favoring the concentration of stresses in this region, allowing plate tectonic forces to play a key role in the process.

Conclusions

Conventional extensional processes, like the idea of a triple junction generated by a mantle plume beneath Northeast Brazil and West Africa, can not explain the kinematics and rift geometry of the Equatorial South Atlantic basins. This region encompass a series of rift basins that were located at and associated with the orthogonal intersection of the Southern and Equatorial branches of the Atlantic rift system. There is no evidence for three synchronous-symmetrically-oriented rift arms. There are major differences between the transform and the divergent margin segments of the South Atlantic. In the divergent segment of the margin (Southern branch) rift architecture is defined by typical rift basins, mainly controlled by the basement structural framework. However, these features are not promptly recognized in the Equatorial margin domain, where the basins were controlled by active strike-slip faulting and wrench tectonics. A key feature is the Transversal Zone, quite orthogonal to the proto-Equatorial Atlantic, and responsible for overcoming the last tectonic link between Africa and Brazil, when simultaneous deformation took place on the northern tip of the southern branch and the Equatorial branch, leaving behind two aborted and diachronous rift arms: the Benue and the onshore Potiguar basin.

Voluminous magmatism clearly post-dated the opening of the Equatorial Atlantic and it is unfavorable to the idea of active rifting as the causal processes for rifting. The tectonic evolution of the sedimentary basins along the Equatorial Atlantic was clearly controlled by the emplacement of the proto mid ocean ridges, followed by the creation of oceanic crust and the onset of transform shearing between Africa and Brazil. Their evolution was related to the kinematic influence of the St. Paul, Romanche and

Chain Fracture Zones, in a classical example of a transform margin.

References

Burke K. and J. T. Wilson, 1976, Hot spots on the earth´s surface. Scientific American, v. 235, p. 46-57.

Matos, R. M. D. de, 1999a, Tectonic Evolution of the Equatorial South Atlantic. Atlantic Rift on Continental Margins, AGU –Geophysical Monograph 115. W. Mohriak and M. Talwani, Editors. 354p.

Matos, R. M. D. de, 1999b, History of the Northeast Brazilian Rift System: Kinematic implications for the breakup Brazil and West Africa. Geol. Soc. Spec. Pub.153, N. Cameron, R. Bate e V. Clure, Ed,.474 p.

O'Connor, J. M., and R. A. Duncan, Evolution of the Walvis Ridge-Rio Grande Rise hot spot system: Implications for African and South American plate motions over plumes. J. Geophys. Res., 95, 17,475-15,502, 1990.

Popoff, M., Du Gondwana à l'Atlantique sud : les connexions du fossé de la Bénoué avec les bassins du Nord-Est brésilien jusqu'a l'ouverture du golfe de Guinée au Crétacé inféreur, In : The West African Connection. In: Sough J. and Rodgers J. (eds) J. Afric. Earth Sci., Spec. Pub., Oxford, G.B. 7, 2, 409-431, 1988.

Vail, J. R., Ring complexes and related rocks in Africa, Journal of African Earth Science, 8, 19-40, 1989.

Wilson, M. and R. Guiraud, Magmatism and rifting in Western and Central Africa, from Late Jurassic to recent times, Tectonophysics, 213, 203-225, 1992.

Acknowledgments:The author is grateful to Petrobras for the opportunity to work on so many Brazilian basins through my years in the company.

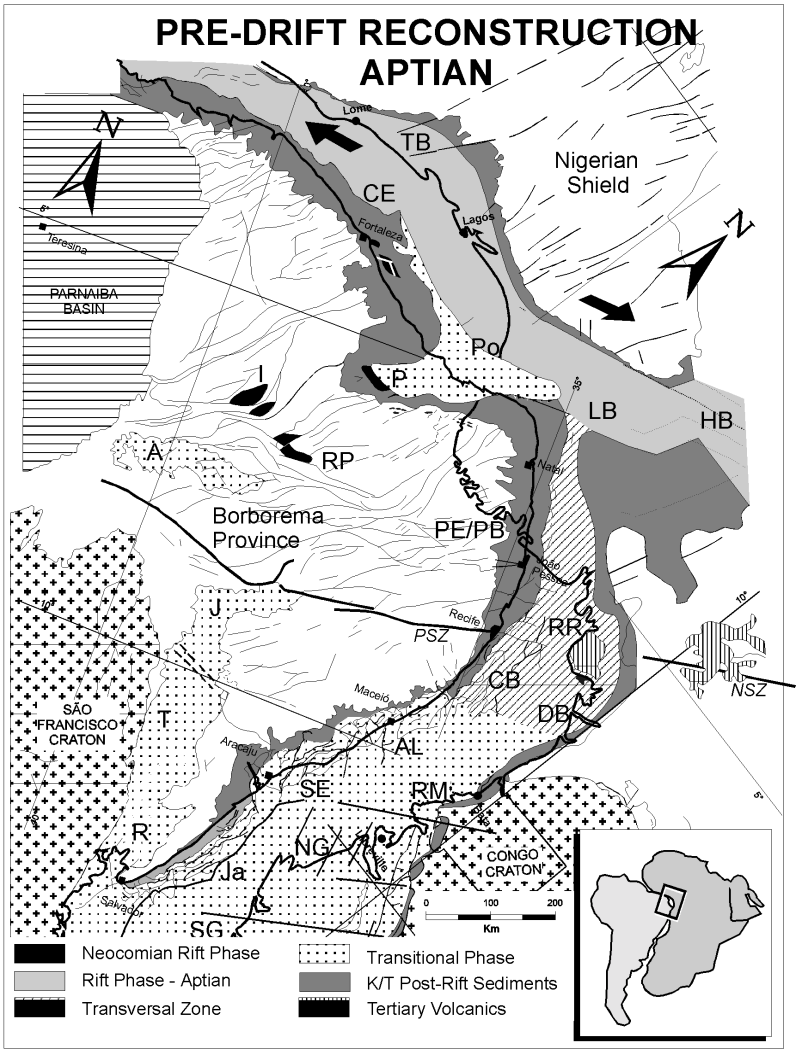

Figure 1. Aptian-pre-drift reconstruction: Paleogeography and the spatial distribution of rift basins immediately prior to break-up of the South Atlantic. The large arrows indicate the direction of tectonic transport in the Equatorial Branch.
African Basins:
TB- Togo Benin
LB - Lower Benue
HB - Higher Benue
RR - Rio del Rey
DB - Douala
RM - Rio Muni
NG - N. Gabon
SG - S. Gabon
Shear Zones:
NSZ - Nagaoundere
PSZ - Pernambuco
Brazilian Basins:
R - Recôncavo
T - Tucano
J - Jatobá
SE - Sergipe
AL- Alagoas
CB - Cabo
P - Potiguar
CE - Ceará
RP - Rio do Peixe

GEODYNAMIC EVOLUTION OF THE SOUTHERN BRANCH

STAGE	KINEMATIC / DYNAMIC	EVENTS	AGE	PHASE
PRE - RIFT	PRE-EXTENSION	Rifts in the Central and in the Southern Atlantic	early Jurassic	Pre-Stretch.
SYN - RIFT	Elastic response of the upper crust to ductile subcrustal stretching and thinning	African-Brazilian Depression and the Rio Ceará Mirim Magmatism	late Jurassic (Tithonian)	Syn-Rift I
	Main rift stage Diffuse continental rifting NW-SE Tectonic Transport	Opening of the Reconcavo -Tucano-Jatoba (RTJ) and Gabon-Sergipe-Alagoas (GSA) rift valleys	early Berriasian	Syn-Rift IIa
	Main rift stage Diffuse continental rifting NW-SE Tectonic Transport (now over 600 km wide)	Extension jumped westward, from the RTJ - GSA trend to the Cariri-Potiguar rift valley (CP).	late Berrias. Barremian	Syn-Rift IIb
	Major change in rift kinematics E-W extension	Main rift stage in the GSA trend, CP aborted, Rifting Benue e Offshore Potiguar. Stretching- Equatorial M.	late Barrem. early Aptian	Syn-Rift III
POST - RIFT	Marine Influence	Transitional Evaporitic Megasequence (GSA-Rio Muni)	Aptian	Transition
	PASSIVE MARGIN	Almost continuous sedimentation as the result of cooling-thermal contraction of the lithosphere	Albian to Recent	DRIFT

Table 1. Geodynamic evolution of the Southern Branch - South Atlantic considering events that predate, are synchronous or posdate rifting

GEODYNAMIC EVOLUTION OF THE EQUATORIAL BRANCH

STAGE	KINEMATIC / DYNAMIC	EVENTS	AGE	PHASE
PRE TRANSFORM	PRE-TRANSTENSION	Rifts in the Central and in the Southern Atlantic (Marajó and Potiguar grabens, respectively)	PRE-BARREMIAN	PRE - STRETCHIN
	SYN-TRANSTENSION	Transtensional conditions created a series of NW-SE trending enechelon depo-centers throughout the Equatorial domain	BARREMIAN TO APTIAN	STRETCHIN
SYN TRANSFORM	PURE-SHEAR DOMINATED TRANSTENSION	Deformation characterized by broad regions dominated by extension, limited by discrete shear zones	ALBIAN TO CENOMANIAN	WRENCH
	WRENCH DOMINATED TRANSTENSION	The divergent movement was accommodated by relatively narrow zones, accounting for most of the the slip between Africa and Brazil		
	WRENCH DOMINATED TRANSPRESSION	A large transpressive belt (Tiaui-Acaraú and Accra basins) as the result of an overall shortening and up-lift around a restraining bend of the Equatorial Atl.		
	PASSIVE TRANSFORM MARGIN	Oceanic/continental crust contact through an active Transform Fault	CENOMANIAN TO RECENT	DRIFT
POST TRANSFORM	PASSIVE MARGIN	Almost continuous sedimentation as the result of cooling-thermal contraction of the lithosphere		

Table 2.. Geodynamic evolution of the Equatorial Atlantic considering events that predate, are synchronous or posdate the activation of transform faults.

Sequence stratigraphy, facies analysis and paleoceanographic events of the Neogene deep-water section in the Campos Basin, offshore Brazil.

Author: **Souza Cruz, C. E.** (PETROBRAS/CENPES/TRO and DEPA-FGEL-UERJ)
e-mail: scruz@cenpes.petrobras.com.br

Introduction

The Campos Basin, situated offshore Rio de Janeiro State, around 23 degrees latitude south, has a total area around 100,000 Km2. It is the most prolific basin in Brazil, with more than five giant oil fields, of which at least four produce in Neogene reservoirs.
This work was carried out in a thick deep-water sedimentary section developed on the basin slope during the Neogene and Upper Oligocene, using 3D seismic sections, well log correlations, cored facies analyses, nanofossil biozones and paleoecology (fig. 1).

Objective

The main purpose of this work is to present: (1) a new interpretation of deep-water deposits that considerably changes previous concepts on this subject; (2) the stratigraphic stacking pattern of the Neogene deep-water section on the Campos Basin Slope; (3) the correlation with Global Eustatic Events (Haq *et al*., 1987); (4) the cored facies analysis and facies associations related to deep-water depositional processes; and (5) the correlation of the events identified in the Campos Basin with coeval "South Atlantic Paleoceanographic Events", especially associated with Antarctic Glaciations.

Sequence Stratigraphy

The thick deep water sedimentary section developed on the Campos Basin slope during the Neogene shows a huge sigmoidal geometry in dip-oriented profiles. In this section, cycle boundaries are the key elements of sequence stratigraphy, which can be identified in seismic sections by means of conventional seismostratigraphy, well log correlation and biostratigraphy. Several third-order unconformity events were identified in the studied interval (Souza Cruz, 1995). Despite the correspondence of boundary cycles with the global eustatic lowering, the sequence stratigraphy elements interpreted in deep-water section should not be confused with shallow water elements. This holds true especially with regard to the nature of deep-water wedges and some erosional unconformities associated with them. These wedges consist entirely of deep-water facies with bathyal faunas, differently from the conventional sequence stratigraphy model (Posamentier *et al*., 1988), (fig. 1).
The most representative seismic geometries in the Neogene interval are represented by huge sigmoidal bodies that prograde and climb up toward offshore in dip-oriented sections (fig.1). Each sigmoidal body is separated vertically from adjoining bodies through an erosional surface, correlative conformities and onlap surface. During the Miocene, these sigmoidal bodies gradually shifted their preferential directions of progradation from southeast to northeast in response to bottom current dynamics. In core analysis they are represented by rhythmic bioturbated mudstone-marlstone bundles in the distal portion, and bioturbated silty-sandy mudstone, with metric thickness, in the central potion of the body (Souza Cruz and Appi, 1999).

Facies Analysis

The Miocene sigmoid sets overlap a basal sandy interval interpreted as a mixed deep-water system (fig. 1). This comprises a pile of sedimentary rocks originated by gravitational flow and bottom current reworking processes during the late Oligocene and early Miocene. The seismic facies of the basal sandy interval shows high amplitude reflection due to its acoustic impedance when compared to the adjacent hemipelagic deposits. It results in anomalous impedance. The well-log signature of these massive sandstone bodies generally presents a box-like pattern, changing to irregular pattern when associated with sandy mudstone and sandstone interbedded with mudstone.
The deep-water sandstone facies range from conglomerate to sandy mudstone deposited as gravitational mass-flows. They have been interpreted as debris flows, high-density turbidity flows, and less commonly graded, fine-grained sediments formed by low-density turbidity flows (Mutti, 1992). Bottom current reworking facies

are mainly represented by fine-grained sediments that normally present traction structures or intense bioturbation. Deposition of the hemipelagic facies took place in bathyal environments through slow planktonic 'rainfall' on the sea floor along with deposition of the terrigenous (silty-clayey) fraction, both subject to bottom current action of variable intensity (Stow and Fougères, 1993).
The hemipelagite and bioturbated sandy-silty mudstone facies are the main constituents of deep-water sigmoidal wedges. Because their deposition was submitted to the action of bottom currents, these sigmoids must be considered as contourite drifts.

Paleoceanographic Events

Eustatic sea-level changes play important role in the origin of deep-water wedges and major erosional unconformities; they are explained by changes in oceanic circulation pattern modulated by climatic changes. The Neogene deep-water section of the Campos Basin clearly records some important paleoceanographic events of the South Atlantic. For instance, the Oligocene- Miocene boundary corresponds to a period of intense global deep-water marine circulation brought about by the Circumpolar Antarctic Current, originated by the opening of the Drake Passage. Coeval events in the Campos Basin include a regional deep-water unconformity and extensive reworking of deep-water sandstones. Two other great deep-water unconformities in the Campos Basin, of middle Miocene (~16.5 Ma) and late Miocene (between 5.5 and 8.2 Ma) ages, correlate respectively with the well known East and West Antarctica glaciations (Souza Cruz, 1995). This demonstrates that Neogene erosional and depositional events in the Campos Basin were controlled by the intensity of bottom currents, the sediment supply/dispersal ratio, and the interaction of bottom currents with the basin morphology.

Bibliography

HAQ, B.U.; HARDENBOL, J.;VAIL,P.R. 1987. Chronology of fluctuacting sea levels since the Triassic. Science, v.235, p.1156-1167.
MUTTI, E. 1992. Turbidite Sandstones. Agip, Milano, 275 p.
POSAMENTIER, H.W.; JERVEY, M.T.; VAIL, P.R. 1988. Eustatic controls on clastic deposition I – conceptual framework. In: Wilgus,C.K.; Hastings, B.S.; Ross, C.A.; Posamentier, H.W.; Van Wagoner, J.C.; Kendall, C.G.St.C. (Eds.), Sea level Changes: an integrated approach: SEPM Special Publication 42, p.109-124.
SOUZA CRUZ, C. E. 1995. Estratigrafia e sedimentação de águas profundas do Neogeno da Bacia de Campos, Estado do Rio de Janeiro, Brasil. Tese de doutoramento, UFRGS, Porto Alegre, RS., 186p.
SOUZA CRUZ, C.E. & APPI, C.J., 1999. Distribution Pattern and Sedimentation of the Neogene Deep Water Section in the Campos Basin, Offshore Brasil. 6th International Congress of the Brasilian Geophysical Society. Rio de Janeiro, Brazil. Extended Abstract (3 pag.).
SOUZA CRUZ, C. E. and APPI, C. J., 2000. Stratigraphy and Sedimentation of the Neogene Deep-water Section in the Campos Basin, Offshore Brazil. International Congress of Geology. Poster Section, Rio de Janeiro, Brazil.
STOW, D.A.V.; FAUGÈRES, J.C., Eds. 1993. Contourites and Bottom Currents, Sedimentary Geology, v.82,n.1-4, 310 p.

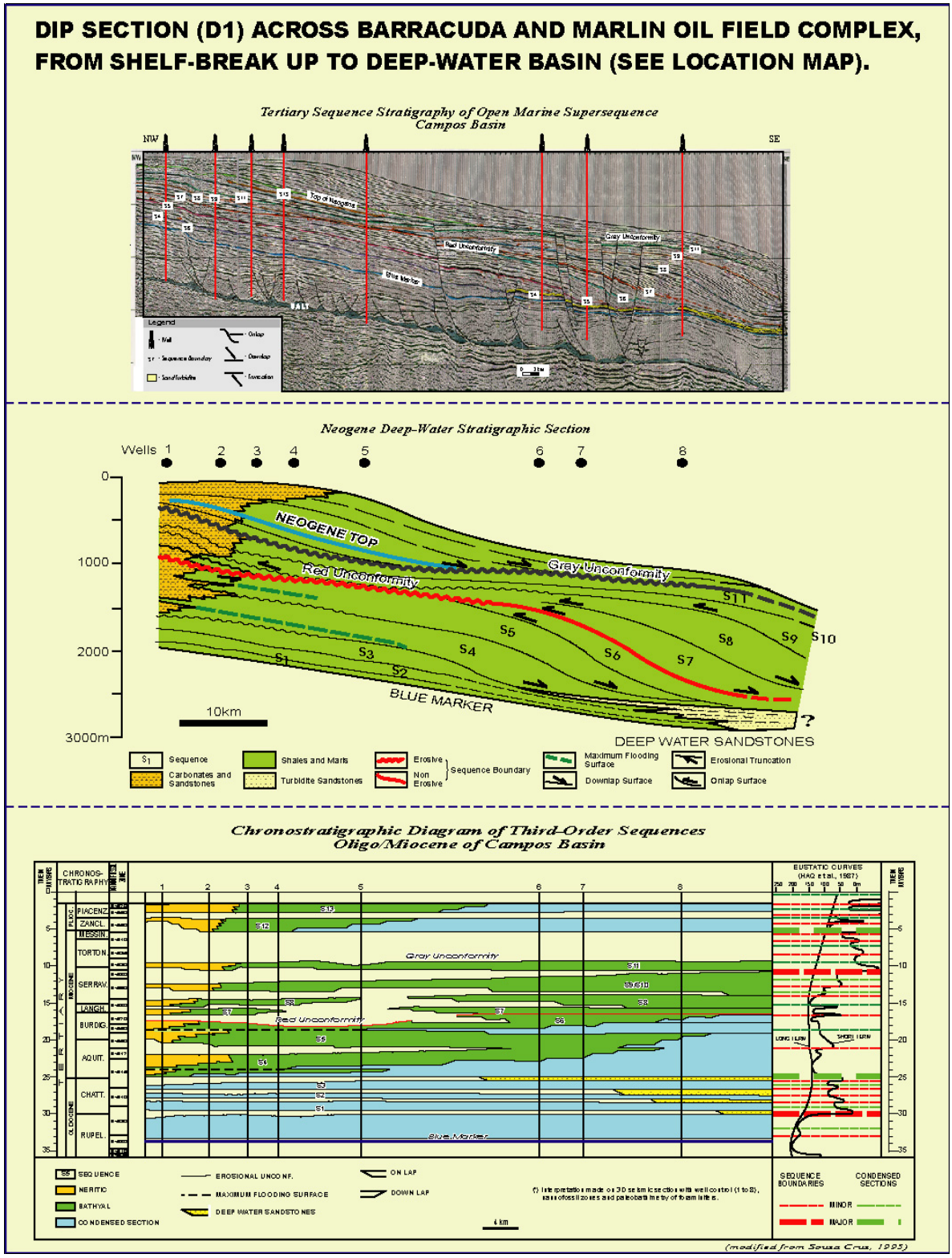

Fig. 1- Interpreted seismic section composed with Neogene stratigraphic section and chonostratigraphic diagram.

Offshore Brazil Santos Basin exploration potential from recently acquired seismic data

Roberto Fainstein, George Jamieson, Andrew Hannan, Norman Biles, Ana Krueger, WesternGeco, Dianna Shelander, Consultant*

Summary

The deep and ultradeep water regions offshore east Brazil is increasingly attracting attention from exploration and production companies. Brazil hydrocarbon production is derived mainly from the giant deepwater fields of the Campos Basin. By contrast, the deepwater regions of the, adjacent to the south, Santos Basin have remained largely under-explored. In actuality, Santos Basin is one of the largest under-explored basins of the world. In the last two decades, there have been several significant discoveries in the southern portion of Santos Basin mainly on carbonate reservoirs. Recently in 1999 a significant discovery occurred on Upper Cretaceous turbidite reservoirs in deepwater. This paper outlines the encouraging hydrocarbon potential of the deepwater realm of Santos Basin by utilizing a recently acquired, processed and interpreted 2D dataset which has revealed numerous, largely untested, play types. These plays include both structural and stratigraphic components. Salt-related large 4-way closures, including faulted and unfaulted turtle structures and drapes over salt have been identified along with sub-unconformity traps. All these identified play types have examples with associated amplitude anomalies, which are widespread throughout the basin, at varying stratigraphic and structural levels.

Introduction

Offshore Brazil's main oil-producing province is in the deepwater Campos Basin and accounts for 70% of Brazilian daily output. Its main oil fields, Marlim, Albacora and Roncador make up more than 50% of the Brazilian proven reserves and Marlim itself makes for more than half of the daily production output. Reservoirs in these deepwater fields are turbidites that range in age from Upper Cretaceous to Miocene. The other offshore producing basins such as Santos, Espírito Santo, South-Bahia, Sergipe-Alagoas, Potiguar and Ceará have so far contributed only a small percentage of total daily output.

.

In the Santos Basin, a significant oil discovery occurred in 1999 in the ultra deepwater region of North Santos Basin on an Upper Cretaceous turbidite reservoir. This discovery has been confirmed by further delineation drilling and has opened a new fairway of turbidite reservoir plays along North Santos Basin. Prior to this discovery, the known oil and gas fields of Santos Basin were the mid-size carbonate fields situated in the southern portion of the basin. These fields, Coral, Tubarão, Estrela do Mar and Caravelas presently produce the bulk of oil of Santos Basin and they are all within BS-3 Block, the deep-water potential of carbonate reservoirs in this block is presently being tested by an exploration well. The only producing gas field in the Santos Basin is the Merluza gas field situated, along the shelf, in central portion of the basin. The deepwater potential of Santos Basin is underscored by the location of its deepwater blocks. In the third bid round of June 2001 all the newly assigned blocks are in ultra deepwater.

Database

In offshore Brazil, modern 2D and 3D seismic data acquisition and processing, both onshore and offshore is dramatically improving data quality and reducing turnaround times. Extremely long streamers, up to 8 km in length, large acquisition footprints, and pre-stack time migration with higher-order normal moveout, are now being increasingly employed. This paper utilizes the largest single 2D survey shot offshore Brazil, namely Brazil '99/2000, a 135,000 line km program covering the Santos, Campos and Espírito Santo Basins. This paper also utilizes a regional structural interpretation carried out on this dataset which also integrated gravity and magnetic data acquired concurrently. In the Santos Basin region these surveys together form a grid of seismic that varies from 8 by 8 km in the southern to 4 by 8 km in the northern Santos Basin.

Brazil '99/2000 surveys were acquired using 8,000-meter streamers. This long cable spread has helped substantially improve the imaging of the deeper section, in particular the lacustrine syn-rift hydrocarbon source section. Imaging of this early Cretaceous stratigraphy is fundamental for a regional understanding of the oil and gas plays. Prestack time migration has been applied to these surveys. This has also greatly improved imaging of salt-sediment interfaces and the delineation of turbidite fans, the major reservoirs in the deepwater petroleum system of the Santos Basin. Publicly available data from 8 wells has also been tied into the seismic over the Santos basin.

Regional Setting

Santos Basin extends from the Cabo Frio volcanic high offshore Rio de Janeiro, to offshore Florianópolis. The area of this basin is approximately 210,000 km^2, making it one of the largest, prospective, under-explored basins in the world (Figs.1 and 2). The continental shelf region of the Santos Basin is wide, reaching 180 km in places. Near the coast, the basin is a platform area that includes the margin hinge line system (Asmus, 1975), generally parallel to the coastline.

In the northern and central Santos Basin lies the Cabo Frio fault zone, consisting of a massive structural collapse of strata near the shelf-break, a result of rapid progradation of the mid-Albian to Late Cretaceous deep water fans onto a thick mobile salt sheet. The progradation of the fans caused the salt mass to be displaced eastwards towards deep water creating a gap in the Albian carbonate section, an absence of Albian age sediments in this region associated with over 50 km of horizontal displacement. Salt that deposited in the rift basin now occupied by the Cabo Frio Fault Zone has been displaced eastwards. The extension seen in the fault zones are balanced by compressional features in the salt ridges.

Massive salt diapirs and walls are abundant in the Santos Basin, locally attaining thickness of over 8 km, particularly in deepwater. These can preclude hydrocarbon migration from

the syn-rift source rocks into the Upper Cretaceous and Tertiary reservoirs. Halokinesis is also intense close to the continental/oceanic crustal boundary. This transitional boundary is sometimes characterized by the occurrence of seaward-dipping reflectors in the central Santos Basin. The distribution of salt in the Santos Basin (Figure 1) shows the progressive thickening of the salt wall into ultra deepwater. This characterizes the São Paulo Plateau, a high basement block that forms the eastern margin of the Santos Basin (Leyden et al., 1978). This plateau is a horst block with more than four kilometers of vertical relief.

There are four distinct depositional environments within the Santos Basin:
1) Continental red shales and conglomerates of the pre-rift sequence.
2) Fine-grained lacustrine sandstones, some of which may form potential reservoirs, and hydrocarbon-rich source rock shales of the syn-rift sequence.
3) Halite, anhydrite and carbonate deposits of the Albian evaporitic sequence deposited during restricted ocean circulation south of the equatorial South Atlantic.
4) Marine sequence including shallow platform carbonates and deeper open marine clastics that contain the recent large deepwater turbidite discovery.

Tectonic Evolution and Stratigraphy

Neocomian-Barremian

Volcanic basement may have been uplifted by a thermal event. The stratigraphic column of the Santos Basin includes a rift phase above early Cretaceous volcanics. Our data suggests that the São Paulo Plateau is separated from the Brazilian Shield by a rift basin. There is a thick rift section at the base of the present day slope. This section is located below the base of the Aptian salt and above the Barremian volcanic basement. Barremian, Guaratiba Fm. lacustrine source rocks were deposited into the early rift valleys that formed Santos Basin. Anoxic conditions existed in the deep parts of the rift valley lakes these preserved the organic rich matter in the source rock. Rocks with up to 10% TOC may have been deposited within these conditions. The thickest source rock section occurs in troughs beneath the present shelf and on the west side of the São Paulo Plateau, generally corresponding to low gravity anomalies. The Barremian section is presently thin or absent over the crest of the São Paulo Plateau, however it is still represented at its flank.

Aptian

The Rio Grande Rise is genetically connected to the Walvis Ridge. The ridges cut off the South Atlantic Ocean water circulation from the south. A source of marine water, probably from the north, provided enough ocean water to evaporate and fill the rift valleys with salt, (Bate, 1999). Santos Basin being farthest from the northern marine source has a very thick, 6 to 7 km, salt field to the east of the São Paulo Plateau (Fig. 1). The successful spreading system developed into the ocean to the east of the plateau. The very thick salt (Ariri Fm.) seen to the east of the plateau is evidence of extensive evaporation and rift fill by the salt.

The salt wall of the Santos Basin formed as Aptian salt filled the failed rift valley between the Brazilian Shield and the offshore São Paulo Plateau.

Albian

Above the Aptian evaporite layers there is a dolomitized section of Albian carbonates. The transition to an open marine environment is marked by a widespread limestone platform in the early Albian. These grade from a shallow marine to a deepwater depositional environment by Cenomanian time.

A passive margin phase characterized by Albian carbonates and also the very thick late Cretaceous siliciclastic succession After the salt's deposition as horizontal layer filling, Aptian rift valleys were covered by a thin continuous sheet of hallow water carbonates. Shallow water marine conditions existed in most of what is now the Santos Basin. Thermal cooling of the Late Albian ocean crust caused subsidence to become very pronounced after Mid Albian. The section tilted down to the east towards the ocean basin.

Albian carbonate rocks are thicker on the present shelf because shallow water favored the production of carbonate material, which were then deposited as a prograding carbonate bank. The carbonates are thinner down dip and offshore into what would have been deeper water, Albian Ocean to the east; however, Late Albian carbonates thicken again farther offshore on the flanks of the São Paulo Plateau. This indicates that the São Paulo Plateau was in shallow water at least through the end of the Albian. There is evidence that some of the carbonates tried to keep up with the thermal subsidence of the São Paulo Plateau by building carbonate mounds and reef like features.

The Cabo Frio fault is a prominent feature on the slope of the Santos Basin. It formed as a counter regional fault. High rate of deposition on the Mid Albian slope displaced Aptian salt to the east. In depth, the salt was pushed up-dip of the west flank of São Paulo Plateau. There are numerous overthrust faults that are thrusting towards the east as a result of the sediments loading the slope and sliding on the plastic salt layer.

The Albian of South Santos basin shows several rollover fault trap anticlines in the Albian carbonate. There appears to be an up dip rim fault where the salt pinches out. The rollover anticlines are apparently caused by the carbonate mounds. Furthermore, the faulting probably provides fractures in the carbonate that aids in the hydrocarbon production of Tubarão, Coral, Estrela do Mar and Caravelas fields. These fields are all located between the salt edge at east and the salt area at west. The salt edge terminates against listric faults.

Turonian-Cenomaniam

Continental terrigenous sediments were deposited on the shelf, and turbidite sandstones cascaded down slope to create a massive slope fan distributary system through the salt basin. Merlusa gas and condensate field in BS-1produces from Turonian sands that pinch out onto the crest of a salt ridge. The trap is partly structural and partly stratigraphic in deep-water turbidite sands.

Santonian-Campanian-Maastrichian

In the drift phase, the large sediment supply from the Serra do Mar mountain range exceeded the accommodation space created by sea level rise and established a prograding section deposited mainly during Campanian/Maastrichian time. This section includes the fluvial and deltaic sediments of the Juréia/Santos Fm. that advanced kilometers beyond the present shelf edge (Pereira et al., 1986).

The shallow shelf to deep-water slope continues to the present. Continental sandstones develop on the shelf, and deep water turbidite sandstone are deposited on the slope in the distributary channel sands, through the salt basin, and are deposited on the flank of the São Paulo Plateau. Most of the growth along the Cabo Frio Fault was generated during this time. The entire Late Cretaceous section thins out over the São Paulo Plateau mostly near the crest. The stratigraphic section pinches out about the flank. Numerous direct hydrocarbon indicators, DHI, occur in the pinch out of the Late Cretaceous section where it onlaps the São Paulo Plateau. Many of the deep-water blocks of Round 2 and many of the blocks available for Round 3 have extensive indications of Upper Cretaceous bright-spots at these stratigraphic levels.

Oligocene

In the Oligocene section there is a pervasive seismic marker the Blue Marker horizon that corresponds to a transgressive event in the Campos Basin. This Oligocene marker may be tied into North Santos Basin where it reveals several thick Oligocene depocenters. Oligocene section, however, is thinner in the Santos Basin as opposed to a generally thicker section in the Campos Basin. The section is thick away from the São Paulo Plateau, and it is thin over the Cabo Frio Fault where the Late Cretaceous sediments filled the basin. There is a thick trough of Oligocene section to the south and west of the São Paulo Plateau. There is also a thick, channeled slope-fan section in this trough extending to the south.

Volcanic Intrusives

Volcanic episodes occurred in late Cretaceous and early Tertiary time, particularly in the northern Santos Basin near Cabo Frio. These volcanic episodes are known in the Santonian (about 84 Ma) and particularly in the Eocene (about 50 Ma) forming moundlike features in the Santos basin.

Petroleum Systems

There are two distinct petroleum systems known in the Santos basin:

1) The Barremian-Maastrichtian, Guaratiba-Ilha Bela system is identified in the northern part of the basin and is related to large but sub-commercial oil fields with biodegraded heavy oil trapped in late Cretaceous to Tertiary siliciclastic turbidite reservoirs (Mohriak et al., 1995). This system is also related to the light oil Upper Cretaceous discovery on the BS-500 Block (Fig.2).

2) The Albian, Guarujá-Guarujá petroleum system is typified by the Tubarão Oil Field and the other fields in the southern portion of the basin, where Albian limestones reservoirs were structured by listric fault blocks and Salt tectonics (Mohriak et al., 1995; see Fig.2).

Plays

The seismic data has brought to light a number of potential deepwater untested plays in this basin. These include; faulted potential 4-way closures; truncations against large salt diapirs, sometimes overhanging; truncations beneath the top Cretaceous unconformity; closures, both faulted and unfaulted, in drapes over salt; large salt withdrawal turtle structures; and stratigraphic pinchouts. All of these plays have examples with associated amplitude anomalies (Fig 3).

For these plays to be viable there are a number of key factors, which must be present. Firstly there must be a nearby well-developed source section. This is typically identified seismically by low frequency, high continuity reflectors below the salt. Another important factor is the ability of the hydrocarbons to migrate through the salt interval and into the reservoir section above. This is best achieved with the presence of thin or welded salt, and can be augmented by large faults, which can occasionally breach the salt (Fainstein, 1999). The recent seismic data used in this study clearly shows the locations of the thicker source sections below the salt.

The São Paulo Plateau is surrounded by numerous deep rift valleys that are probably source rock rich. In this region, deepwater turbidite sands pinch-out against the flanks of the salt. Hydrocarbons may have migrated updip from basin lows to the structural highs from west to east. The São Paulo Plateau was probably exposed during Early Albian to Late Cretaceous and large carbonate banks may have developed that are now located within the present day ultra deepwater realm.

Widespread massive salt walls occur over a large extent of the Santos Basin. The prospects around the salt wall, in the intervening mini-basins, consist of terminations of turbidite beds of Upper Cretaceous age against the salt wall. This play, is still untested, due to economics and uncertainties about salt

versus sediment stratification in the mini-basins. The new seismic dataset has significantly improved imaging of the well-developed syn-rift sections that suggest new plays in prospective reservoirs in the early Cretaceous Guaratiba, such as the coquinas of the Barremian/Early Aptian, and also in lacustrine sandstones.

Conclusions

Our study of Santos Basin (Fainstein et al., 2001), based on recently acquired data, has identified a slew of new plays in the Santos Basin in deep and ultra deepwater. These if proven to fruition would then establish Santos Basin as a future significant hydrocarbon producing province in deepwater. Proven, producible, oil bearing deep-water reservoirs have been recently uncovered in Upper Cretaceous turbidite sequences in the northern and central Santos Basin. The older central Santos Merluza gas discovery is now developed, and the newest deepwater discovery in the northern Santos BS-500 block has been confirmed by recent delineation drilling. These turbidite plays add to the producing Albian carbonate reservoirs in the southern Santos Basin that continues to be a significant reservoir target with further exploratory and development drilling now taking place in and around Block BS-3. Plays have also been identified in salt bounded mini-basins of Upper Cretaceous age and also within the syn-rift section. These have been possible by our pre-stack depth imaging of the syn-rift section and by our high-resolution imaging of U. Cretaceous.

Acknowledgements

The authors thank WesternGeco and TGS Nopec for display of seismic data of the Brazil '99/2000 program.

References

Asmus, H.E., 1975, Contrôle estrutural da deposição mesozóica nas bacias da margem continental brasileira, Revista Brasileira de Geociências, v.5, p. 160-175.

Bate, R. H., 1999, Non-marine ostracod assemblages of the Pre-Salt rift basins of West Africa and their role in sequence stratigraphy, In: Cameron, N.R., bate, R. H. & Clure, V. S. (eds) The Oil and Gas Habitats of the South Atlantic. Geological Society, London, Special Publications, 153, 283-292.

Fainstein, R., 1999, Brazil Expands Exploration of its twenty Offshore Sedimentary Basins, Pennwell Offshore Magazine, October, p. 56-60.

Fainstein, R., Jamieson, G.A., Biles, N., Hannan, A.E., Shelander, D.L. and Krueger, A.C.V.A., 2001, Brazil 99/2000 – Regional Interpretation Report, Schlumberger (unpublished), 108 pp.

Leyden, R., Damuth, J.E., Ongley, L.K., Kostecki, J. and Van Stevenick, W., 1978, Salt Diapirs on São Paulo Plateau, Southeastern Brazilian Continental Margin, AAPG Bulletin, v.62, no.4, p. 657-666.

Mohriak, W.U., Macedo, J.M., Castellani, R.T., Rangel, H.D., Barros, A.Z.N., Latge, M.A.L., Ricci, J.A. and Aires, J.R., 1995, Salt tectonics and structural styles in the deep water province of the Cabo Frio region, Rio de Janeiro, Brazil, in M.P.A. Jackson, D.G. Roberts and S. Snelson, eds, Salt tectonics: A global perspective: AAPG Memoir 65, p. 273-304.

Pereira, M.J., Barbosa, C.M., Agra, J., Gomes, J.B., Aranha, L.G.F., Saito, M., Ramos, M.A., Carvalho, M.D., Stamato, M, and Bagni, O., 1986, Estratigrafia da Bacia de Santos: análise das sequências, sistemas deposicionais e revisão litho-estratigráfica; Congresso Brasileiro de Geologia, 34, Goiânia, v.1, p. 65-79.

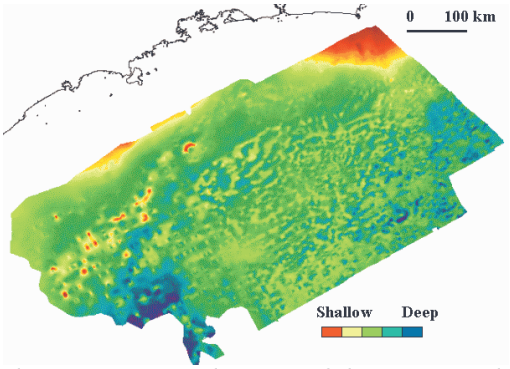

Figure 1: Two-way-time map of the Santos Basin top salt horizon

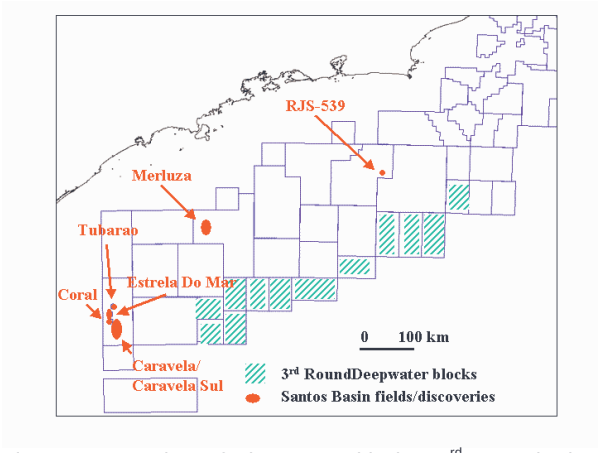

Figure 2: Location of deepwater blocks, 3rd Round ultra deepwater blocks (green shade) and fields and discoveries of the Santos Basin

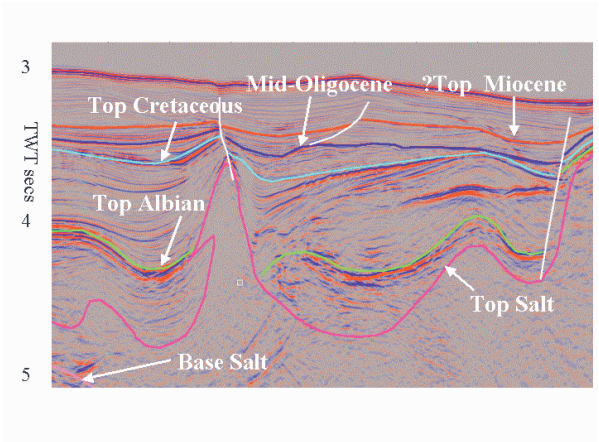

Figure 3: Interpreted seismic section showing large drape structure with associated amplitude anomaly over deep salt and truncations beneath Cretaceous unconformity